

Ga-doped Czochralski silicon with rear p-type polysilicon passivating contact for high-efficiency p-type solar cells



Yuyan Zhi^{a,b}, Jingming Zheng^{b,c}, Mingdun Liao^b, Wei Wang^b, Zunke Liu^{b,c}, Dian Ma^b, Mengmeng Feng^b, Linna Lu^{b,c}, Shengzhao Yuan^d, Yimao Wan^d, Baojie Yan^{b,c}, Yuming Wang^e, Hui Chen^e, Meiyi Yao^{a,b,**}, Yuheng Zeng^{b,c,*}, Jichun Ye^{b,c,***}

^a Institute of Materials, Shanghai University, Shanghai City, 200072, PR China

^b Ningbo Institute of Material Technology and Engineering, Chinese Academy of Sciences, Ningbo City, Zhejiang Province, 315201, PR China

^c University of Chinese Academy of Sciences, Beijing, 100049, PR China

^d Risen Energy Co., Ltd, Ningbo City, Zhejiang Province, 315609, PR China

^e Suzhou Tuosheng Intelligent Equipment Co., Ltd, Suzhou City, Jiangsu Province, 215156, PR China

ARTICLE INFO

Keywords:

Ga-doped CZ-Si
p-type passivating contact
TOPCon
Light-induced degradation

ABSTRACT

The use of Ga-doped Czochralski (CZ) silicon wafers in Passivated Emitter and Rear Cells (PERC) has been confirmed to have a prominent advantage in suppressing light-induced degradation (LID), which will attract considerable attention for the application of Ga-doped wafers in more efficient photovoltaic devices. In this work, we investigate the passivation quality and address the issue of LID in Ga-doped CZ Si wafers equipped with p-type polysilicon passivating contact that consists of an ultrathin SiO_x and a heavily doped polysilicon. We also present the modeling results for solar cells using this type of contact. The experiments show that samples with Ga-doped CZ Si wafers have superior anti-LID properties when compared to the samples with B-doped wafers. An excellent passivation performance with a high implied open-circuit voltage (iV_{oc}) of 705 mV and a low single-sided saturation current density ($J_{0,s}$) of 9 fA/cm² was achieved. Moreover, with the help of the numerical simulations, we predict that the p-type Ga-doped CZ Si solar cells with p-type polysilicon passivating contacts have the potential to achieve a high efficiency of 23.8%, an ~0.5% absolute efficiency improvement over that of PERC solar cells. The results demonstrated in this study suggest that Ga-doped CZ Si wafers combined with p-type polysilicon passivating contacts could resolve the LID issue while maintaining good passivation properties, providing a promising alternative for p-type solar cells in the photovoltaic industry.

1. Introduction

Owing to the presence of B-O pairs, mainstream PERC solar cells with B-doped CZ Si wafers often experience the LID issue [1–4]. If the B acceptors are substituted by Ga in the CZ Si wafers, the LID is mitigated or fully avoided. This concept has been explored and validated. For example, Glunz and Meemongkolkij et al. separately confirmed that Ga-doped CZ Si PERC solar cells have improved light stability compared to B-doped cells [5,6]. Moreover, with the development of Si ingot growth technology, low-cost Ga-doped CZ Si wafers with uniform

resistivity have become available, enabling their wide application in PERC solar cells. Recently, mass-produced PERC solar cells featuring high-quality Ga-doped CZ Si wafers have demonstrated excellent device performance with high and stable efficiencies beyond 23% [7].

Although Ga-doped CZ Si wafers have been successfully introduced into PERC solar cells to alleviate the LID issue, further improvements in the efficiency of PERC solar cells are still limited by the irrepressible carrier recombination losses caused by the direct contact of rear electrodes with Si wafers. To address this issue, polysilicon passivating contact technology consisting of an ultrathin SiO_x and a heavily doped

* Corresponding author. Ningbo Institute of Material Technology and Engineering, Chinese Academy of Sciences, Ningbo City, Zhejiang Province, 315201, PR China.

** Corresponding author. Institute of Materials, Shanghai University, Shanghai City, 200072, PR China.

*** Corresponding author. Ningbo Institute of Material Technology and Engineering, Chinese Academy of Sciences, Ningbo City, Zhejiang Province, 315201, PR China.

E-mail addresses: yaomeiyi@t.shu.edu.cn (M. Yao), yuhengzeng@nimte.ac.cn (Y. Zeng), jichun.ye@nimte.ac.cn (J. Ye).

polysilicon, also known as tunnel oxide passivating contact (TOPCon) or polysilicon on passivating interfacial oxides (POLO), was developed. By employing an ultrathin SiO_x as a high-quality passivation layer and a heavily doped polysilicon film as a carrier-selective contact, TOPCon structures can simultaneously improve the rear-side passivation and carrier collection [8–11]. Additionally, as one of the most promising technologies for the next generation of photovoltaic (PV) industry, TOPCon devices have achieved high efficiencies of >24% in the mass production of n-type solar cells [12,13].

One feasible method to improve the competitiveness of p-type Si solar cells is to adopt a p-type polysilicon passivating contact on p-type Si wafers. Much of the pioneering work related to such structures has been conducted. Feldmann et al. achieved a single-sided saturated current density ($J_{0,s}$) of approximately 50 fA/cm², which is significantly inferior to the $J_{0,s}$ of a n-type polysilicon passivating contact [14]. Mack [15], Young [16], and Stodolny [17] et al. employed a low-pressure chemical vapor deposition (LPCVD) technology to prepare in-situ B-doped polysilicon and achieved an excellent passivation quality with an implied open-circuit voltage (iV_{oc}) of >730 mV and a minimal $J_{0,s}$ of 1–3 fA/cm². Moreover, Yan et al. developed a p-type polysilicon contact using a sputtering technology, achieving a low $J_{0,s}$ of ~16 fA/cm² [18]. Ingenito et al. developed a fast (<10 s) high-temperature (>750 °C) annealing p-type polysilicon contact with a nanocrystalline SiC:H buffer layer using very-high-frequency plasma-enhanced chemical vapor deposition (VHF-PECVD) technology and obtained a low $J_{0,s}$ of ~11 fA/cm² [19]. Continued improvement in device performance results in the potential application of p-type silicon wafers with p-type polysilicon passivating contacts in industry.

In this study, we fabricated p-type TOPCon structures based on p-type Ga-doped CZ Si wafers and p-type polysilicon passivating contacts and experimentally investigated their passivation and light-stability properties. Compared with B-doped and P-doped CZ Si wafers, the Ga-doped CZ Si wafers had notable advantages in terms of annealing temperature tolerance, bulk and surface defects, and LID. As a result, the Ga-doped wafers displayed excellent passivation properties with an optimal iV_{oc} of 706 mV and a low $J_{0,s}$ of ~9 fA/cm² at a minority carrier density (Δn) of 10¹⁶ cm⁻³. Additionally, a numerical simulation was implemented to predict the performance of p-type polysilicon passivating contact solar cells on Ga-doped Si wafers, which suggested a competitive efficiency of 23.8%.

2. Experiment

Three types of alkaline-polished CZ Si wafers with <100>-orientation were used as the substrates, 175-μm Ga-doped p-type CZ Si wafers with doping concentrations of (1.7–2.7) × 10¹⁶ cm⁻³, 175-μm B-doped p-type CZ Si wafers with doping concentrations of (0.9–1.1) × 10¹⁶ cm⁻³, and 165-μm P-doped n-type CZ Si wafers with doping concentrations of (0.09–0.13) × 10¹⁶ cm⁻³. The Si wafers were cleaned using the standard RCA procedure, followed by the removal of native SiO_x by dipping in a diluted HF solution. An ultrathin SiO_x layer was grown on both sides of the Si wafers using plasma-assisted N₂O oxidization (PANO) in a 13.56 MHz PECVD system (FE thin film) [20]. Subsequently, ~40 nm B-doped a-Si:H was deposited in the same PECVD system using silane (SiH₄), hydrogen (H₂), and diborane (B₂H₆) as the reactive gases. The samples bi-facially coated with SiO_x /a-Si:H were annealed at 820–960 °C for 30 min to crystallize the films and activate their dopants. Further hydrogenation was carried out by covering the polysilicon surface with AlO_x grown in an atomic layer deposition (ALD) system (NCD), followed by annealing at 450 °C. The passivated samples were subjected to one-sun (~1000 Wm⁻²) light soaking at 75 °C in a N₂ protective atmosphere for 1200 min (ES-HS-150B).

The passivation quality was characterized by quasi-steady-state photoconductance (QSSPC) measurements (Sinton WCT-120), from which the effective minority carrier lifetime (τ_{eff}), iV_{oc} , and $J_{0,s}$ were extracted. The active dopant distribution profiles were measured using

an electrochemical capacitance-voltage (ECV) system (Buchanan, CVP21). A numerical simulation was performed using Quokka 2 [21, 22].

3. Results and discussion

First, the passivation quality of Ga-doped CZ Si wafers passivated with the SiO_x and polysilicon bi-layer prepared by PECVD was investigated, and the counterparts with B-doped and P-doped CZ Si wafers were also presented as a contrast. All samples were subjected to AlO_x hydrogenation after the preparation of p-type polysilicon layers. Fig. 1 (a–f) show that the annealing temperature exerts a significant influence on the passivation quality for the three kinds of samples (iV_{oc} and $J_{0,s}$ were extracted at $\Delta n = 10^{16}$ cm⁻³). The data points are the average values obtained from the measurements of two or three samples. The iV_{oc} of the B-doped and P-doped samples first increased to reach the optimal values and then started to decrease at higher temperatures, yielding the optimal values at 920–940 °C. In comparison, the iV_{oc} of Ga-doped CZ Si samples increased as the annealing temperature increases from 820 °C to 960 °C, and a high passivation quality of more than 700 mV can be maintained over a high annealing temperature range of 900–960 °C. The Ga-doped samples exhibited a champion iV_{oc} of 706 mV at 960 °C, while which are 705 mV at 920 °C, and 708 mV at 940 °C for B-doped and P-doped samples, respectively. The p-type polysilicon/PANO SiO_x contact on the n-type substrate achieved the best iV_{oc} of 700 mV in our previous work [20], indicating an improved passivation quality in this work. Correspondingly, the minimal $J_{0,s}$ ($\Delta n = 10^{16}$ cm⁻³) of the Ga-doped, B-doped, and P-doped samples were 9.0, 9.8, and 14.0 fA/cm², respectively. In addition, to the best of the author's knowledge, a $J_{0,s}$ of 9 fA/cm² is the lowest value achieved with PECVD-processed p-type polysilicon contact on p-type CZ Si wafers. In our work, the Ga-doped and B-doped samples showed competitive passivation qualities with similar iV_{oc} and $J_{0,s}$. Specifically, the passivated Ga-doped CZ Si wafers with the minimal $J_{0,s}$ of ~9 fA/cm² display a lower electrode contact recombination than the $\text{AlO}_x/\text{SiN}_x$ stack layer in PERC devices, suggesting the potential use of p-type polysilicon contacts for higher efficiency p-type solar cells than the current PERC products.

The effective minority carrier lifetime spectra of the samples with p-type polysilicon passivating contact on the Ga-doped, B-doped, and P-doped Si wafers under their optimal passivation performance are shown in Fig. 2. Three types of passivation structures were used on each of the samples: the AlO_x passivation layer, as-annealed polysilicon/ SiO_x passivating contact, and polysilicon/ SiO_x contact with the capping AlO_x hydrogenation layer. The AlO_x passivated sample is given as a reference because AlO_x hydrogenation provides an excellent passivation and effectively evaluates the intrinsic bulk defects inherent to the p-type wafers. The observations of these results are as follows: 1) The lifetime values of the as-annealed polysilicon passivated samples are the lowest, indicating that the passivation quality of the as-crystallized polysilicon contact case is limited by the inferior interface recombination in comparison with that of the AlO_x capping layer. 2) The lifetime values of the AlO_x -hydrogenated polysilicon contact passivated samples were significantly improved, which provides an opportunity to evaluate the intrinsic defects of bulk Si substrates. 3) The champion lifetime of Ga-doped CZ silicon passivated by polysilicon and AlO_x is 310 μs ($\Delta n = 10^{15}$ cm⁻³), which is higher than that of the B-doped counterpart. 4) It is worth noting that the lifetime values of B-doped and P-doped CZ Si samples decrease with the reduction of the injection level in the low minority carrier concentration zone, which can be well maintained for Ga-doped CZ Si samples. The decrease in carrier lifetime with a decrease in carrier concentration in the low concentration region is mainly attributed to the minority carrier recombination in bulk [23,24] and therefore cannot be enhanced by surface passivation technology. For the B-doped samples, the degradation can be attributed to the bulk-related effect with the activation of B-related complexes [25] or B clusters [26]. In contrast, for P-doped samples, the dominant recombination in

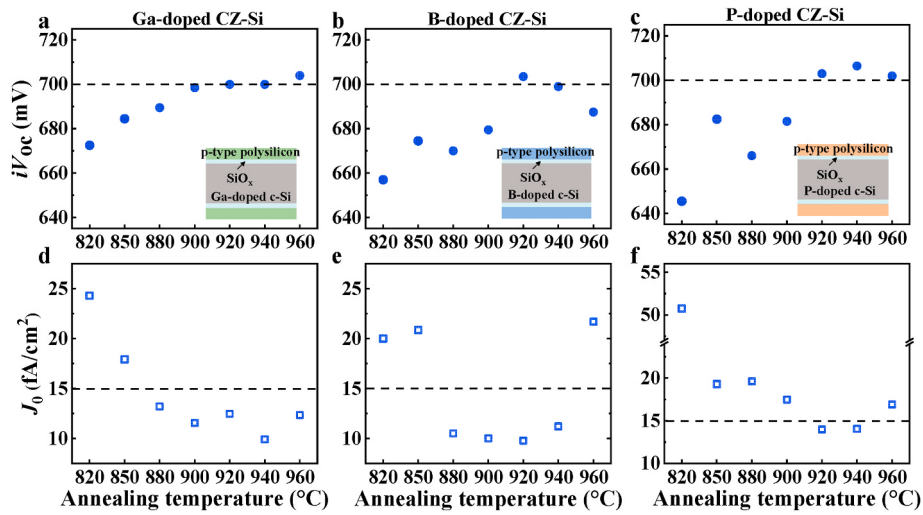


Fig. 1. (a)–(c) iV_{oc} and (d)–(f) $J_{0,s}$ of the three related samples (i.e., Ga-doped, B-doped, and P-doped Si wafers with double-sided p-type polysilicon passivating contact structures) at various annealing temperatures. The $J_{0,s}$ is extracted under $\Delta n = 10^{16} \text{ cm}^{-3}$ for both the p-type and n-type CZ Si samples. All the samples have been hydrogenated through an annealing process of ALD-processed AlO_x layer at 450 °C.

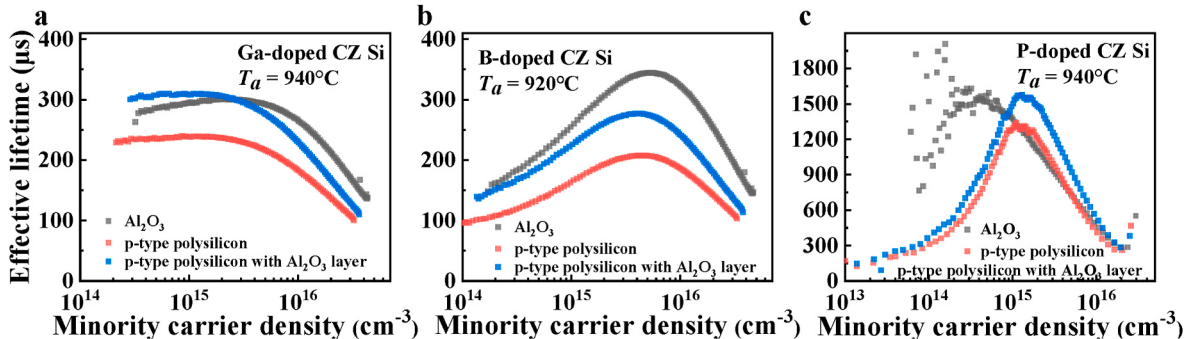


Fig. 2. Lifetime spectra of the (a) Ga-doped, (b) B-doped, and (c) P-doped samples with their respective optimal passivation quality with the three different passivation structures of the AlO_x passivation layer, the as-annealed polysilicon passivating contact, and the polysilicon contact plus the AlO_x hydrogenation layer.

the low minority carrier injection density can be explained by the presence of a space charge region at the p-n junction [27]. However, the explanation for the inhibition of deep-level defects in the Ga-doped wafers has not been revealed yet, and the relative discussion will be presented in the following sections.

The effect of Ga doping on the recombination was also investigated, as shown in Fig. 3. We used bulk saturation current density ($J_{0,\text{bulk}}$) to express the bulk recombination of the passivated samples, which was extracted using the method developed by Müller et al. [28]. We made the following observations. 1) The $J_{0,s}$ values of both B-doped and Ga-doped samples first decreased and then increased slightly as the

annealing temperature increases from 820 °C to 960 °C. The minimal $J_{0,s}$ appeared at 940 °C for both the B-doped and Ga-doped samples. Although the B-doped and Ga-doped samples have similar $J_{0,s}$, the iV_{oc} is typically higher for the Ga-doped samples than for the B-doped samples at most annealing temperatures. 2) The extracted $J_{0,\text{bulk}}$ in Fig. 3(b)–(c), indicates that the bulk recombination of the Ga-doped samples was typically lower than that of the B-doped samples. Further, the extracted $J_{0,\text{bulk}}$ of the Ga-doped samples was typically lower than 80 fA/cm^2 as $\Delta n < 10^{16} \text{ cm}^{-3}$, and the minimal value approached $\sim 40 \text{ fA/cm}^2$ at 960 °C. In contrast, the extracted $J_{0,\text{bulk}}$ of the B-doped samples was more than 100 fA/cm^2 as $\Delta n < 10^{16} \text{ cm}^{-3}$ at annealing temperatures of 880 °C and

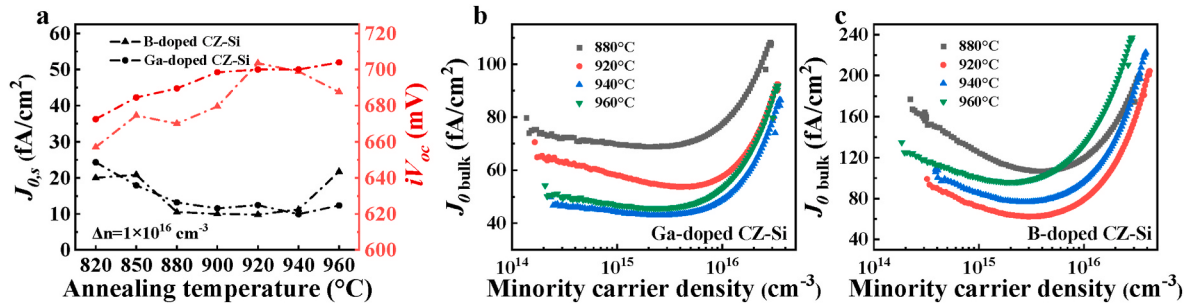


Fig. 3. (a) Influence of the annealing temperature on $J_{0,s}$ and iV_{oc} of the p-type polysilicon passivating contact samples on the Ga-doped and B-doped CZ Si substrates. (b) $J_{0,\text{bulk}}$ of Ga-doped samples as a function of the minority carrier density, and (c) $J_{0,\text{bulk}}$ of B-doped samples as a function of the minority carrier density.

960 °C, and it was reduced to ~60 fA/cm² at an annealing temperature of 920 °C. The extracted $J_{0,\text{bulk}}$ can quantitatively assess the quality of the two wafers. The bulk recombination caused by the quality of Ga-doped wafers was significantly lower, but the surface passivation quality $J_{0,s}$ was similar, so the passivation difference in iV_{oc} (especially under high-temperature annealing conditions from 940 °C to 960 °C) between the two wafers was mainly due to the difference in wafer quality. 3) For the 960 °C high-temperature treatment, the $J_{0,\text{bulk}}$ of Ga-doped CZ Si has the lowest value of ~40 fA/cm². The results presented above indicate that the Ga-doped wafers with p-type polysilicon contact possessed better high-temperature stability and required a higher temperature to achieve optimal passivation.

To further reveal the effect of Ga doping in Si wafers on surface and bulk recombination, the active B-doping concentration profiles of the samples with the three types of wafers were characterized using ECV measurements, as shown in Fig. 4. The observations are as follows: 1) The active B-doping depth in the P-doped Si wafers was always shallower than those in the B-doped and Ga-doped wafers, which is understandable because the diffusion of B was enhanced in B (or Ga)-doped Si wafers with the assistance of majority carriers of holes, but retarded in P-doped Si wafers with the majority carriers of electrons [29–31]. 2) The impact of Ga doping on B-diffusion is not significant because the in-diffusion profiles in the B-doped and Ga-doped CZ Si wafers are almost coincident. Thus, the values of diffusion-induced saturation current densities ($J_{0,\text{diff}}$) are similar in the B-doped and Ga-doped CZ Si wafers for the three reference temperatures. As the active B-doping concentration profiles in the Ga-doped and B-doped CZ Si wafers are similar, the primary reason for the different passivation qualities should be attributed to the Ga-doped CZ-Si substrate but not to the B in-diffusion profile.

The three samples passivated by the as-annealed p-type polysilicon contact were subjected to prolonged one-sun illumination at 75 °C to examine the effect of the doping impurities on the LID. The effective lifetimes under illumination extracted at 10¹⁵ cm⁻³ and the corresponding normalized lifetimes are shown in Fig. 5(a)–(b), respectively. Herein, we employed samples passivated by the as-annealed polysilicon contact to avoid the influence of hydrogen. The sample on the B-doped CZ Si displayed a significant lifetime degradation at the beginning of the one-sun illumination at 75 °C, that is, the lifetime decreased to 40% of the initial value after 40 min of illumination, which is believed to be caused by the B-O pair generation in the B-doped wafers under illumination. In comparison, the lifetime of the P-doped CZ Si samples only displayed slight degradation, that is, the lifetime decreased to 95% of the initial value after 1200 min of illumination. As expected, the Ga-doped sample also manifested a stable lifetime during the extended one-sun illumination at 75 °C, that is, the lifetime was reduced to 98% of the initial value after 1200 min illumination, exhibiting even better anti-LID performance than the P-doped wafers.

From the results presented above, we determined that the Ga-doped

samples have the advantages of high-temperature stability, low bulk recombination, and anti-LID performance. However, the underlying mechanisms remain unclear. Herein, a possible mechanism is proposed to explain the superior performance of Ga-doped Si wafers. The lifetime of the B-doped samples degrades significantly during the high-temperature B diffusion process, which is generally attributed to the generation of B-relative defects, such as B clusters [26] or B-O complexes [3]. In B-doped wafers, the tensile strain generated by the B atom in the Si lattice facilitates the injection of self-interstitial silicon (Si_i) and O_i, leading to the formation of B clusters and BO complexes. In the Ga-doped wafers, the doping of Ga atoms does not contribute to the formation of B clusters and BO complexes because of the much smaller strain caused by Ga atoms. Therefore, there are fewer B clusters and BO complexes in Ga-doped wafers compared to B-doped wafers [32]. Further investigation is required to prove the assumptions presented above.

Finally, to predict the potential efficiencies of this type of solar cell, numerical simulations were performed using Quokka 2. The main input parameters shown in Table 1 were extracted from the experiments in this work or references. Some of the parameters, for example, $J_{0,\text{met}}$ of polysilicon contact, refer to the relative works (F-ISE [33], SERIS [34]). The structures of the solar cells with rear p-type polysilicon passivating contact and rear PERC contact are shown in Fig. 6(a) and (b), respectively. The only difference between the two types of solar cells is the rear-side design. The advantages of the rear p-type polysilicon contact include reduced rear metal-contact recombination and contact resistivity, optimized rear sheet resistance, and improved overall rear surface passivation. Substituting the rear PERC structure with the rear p-type polysilicon passivating contact resulted in a gain in efficiency (η), mainly from V_{oc} and FF . The V_{oc} increased from 686 to 695 mV, and the FF increased from 82.3% to 82.6%. From the free energy loss analysis (FELA), it was determined that the improvement in V_{oc} resulted from the reduction of rear recombination (total rear J_0 reduced from 52.35 to 15.83 fA/cm²), and the increase in FF originated from the reduction of rear resistive loss (rear R_{sheet} reduced from 450 to 30 Ω/sq). Finally, a total absolute efficiency gain of ~0.5% was achieved using the rear p-type polysilicon contact, which is a significant progress for a p-type solar cell. This suggests that Ga-doped CZ Si wafers with p-type polysilicon passivating contact provided a facile scheme for the development of p-type solar-cell technology for the PV industry.

4. Conclusion

In this work, we investigated high-performance PECVD-prepared p-type polysilicon passivating contacts on Ga-doped, B-doped, and P-doped CZ Si wafers. The passivation quality of the samples on the three types of wafers was investigated at different annealing temperatures from 820 °C to 960 °C. The results showed that the passivated Ga-doped CZ Si wafers exhibited an impressive passivation performance at

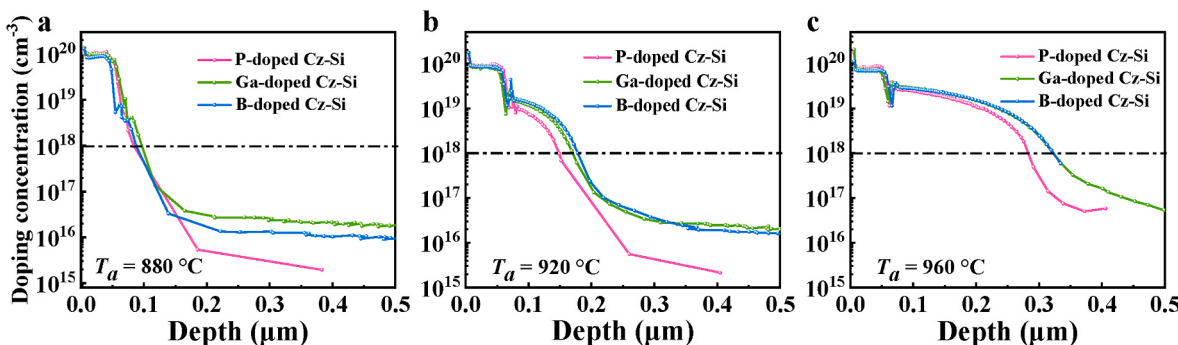


Fig. 4. In-diffusion profiles of active B concentration in the p-type polysilicon passivating contact samples on the Ga-doped, B-doped, and P-doped wafers annealed at (a) 880 °C, (b) 920 °C, and (c) 960 °C.

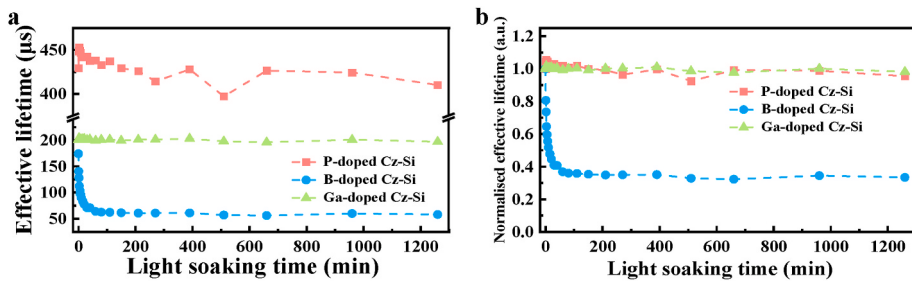


Fig. 5. (a) Effective lifetime and (b) normalized lifetime of the Ga-doped, B-doped, and P-doped samples subjected to one-sun illumination at 75 °C for 1200 min.

Table 1
Parameters for simulations.

Structure	TOPCon	PERC
cell thickness	170 μm	170 μm
p-type bulk resistivity	0.75 Ω cm	0.75 Ω cm
bulk lifetime	1000 μs	1000 μs
auger model	Richter 2012	Richter 2012
generation current	42.57 mA cm ⁻²	42.57 mA cm ⁻²
series resistance	0.1 Ω cm ²	0.1 Ω cm ²
shunt resistance	1 × 10 ⁵ Ω cm ²	1 × 10 ⁵ Ω cm ²
Front side	Line, width 30 μm	Line, width 30 μm
front contact shape		
distance between front fringe	1400 μm	1400 μm
front $J_{0,met}$	800 fA/cm ²	800 fA/cm ²
front $R_{sheet,n+}$	90 Ω/sq	90 Ω/sq
front width of n ⁺⁺	80 μm	80 μm
front $J_{0,n++}$	100 fA/cm ²	100 fA/cm ²
front $J_{0,pas}$	30 fA/cm ²	30 fA/cm ²
front $R_{sheet,n+}$	150 Ω/sq	150 Ω/sq
front contact resistivity	1 mΩ cm ²	1 mΩ cm ²
Rear side	Line, width 30 μm	Line, width 30 μm
rear contact shape		
distance between rear fringe	400 μm	400 μm
rear $R_{sheet,p+}$	30 Ω/sq	450 Ω/sq
rear J_0	9 fA/cm ²	12 fA/cm ²
rear $J_{0,met}$	100 fA/cm ²	550 fA/cm ²
rear contact resistivity	1 mΩ cm ²	2 mΩ cm ²

relatively high annealing temperatures ($iV_{oc} > 705$ mV, $J_{0,s} = 9$ fA/cm²). In addition, the Ga-doped Si samples annealed at higher temperatures (940 °C–960 °C) could maintain their original passivation quality (940 °C–960 °C), whereas their counterparts with B-doped and P-doped

wafers experienced severe passivation degradation. The high-quality passivation properties associated with Ga-doped wafers were analyzed with a focus on the parameters of iV_{oc} , $J_{0,s}$, $J_{0,bulk}$, and effective lifetime. It was demonstrated that the $J_{0,bulk}$ values of samples on Ga-doped wafers were significantly lower than those of B-doped wafers, which was also confirmed from the carrier lifetime spectra. The improvement in carrier lifetime of the Ga-doped samples can be attributed to the inhibition of the generation of B-relative defects such as B clusters and B–O complexes. The LID tests at 75 °C for 1200 min under one-sun illumination also showed that the passivated Ga-doped wafers possessed a significant advantage in anti-LID. The numerical simulations showed an expected efficiency of 23.8% for solar cells based on Ga-doped CZ Si wafers with rear p-type polysilicon passivating contact. These findings suggest that Ga-doped CZ Si wafers with p-type polysilicon passivating contact provide a promising p-type solar cell technology for the photovoltaic industry.

CRediT authorship contribution statement

Yuyan Zhi: Investigation, Data curation, Writing – original draft.
Jingming Zheng: Investigation. **Mingdun Liao:** Investigation. **Wei Wang:** Investigation. **Zunke Liu:** Investigation. **Dian Ma:** Investigation. **Mengmeng Feng:** Investigation. **Linna Lu:** Investigation. **Shengzhao Yuan:** Resources. **Yimao Wan:** Investigation, Resources. **Baojie Yan:** Conceptualization, Resources, Writing – review & editing. **Yuming Wang:** Resources. **Hui Chen:** Resources. **Meiyi Yao:** Formal analysis, Project administration, Supervision. **Yuheng Zeng:** Conceptualization, Formal analysis, Writing – original draft, Writing – review & editing, Project administration. **Jichun Ye:** Validation, Writing – review & editing, Supervision.

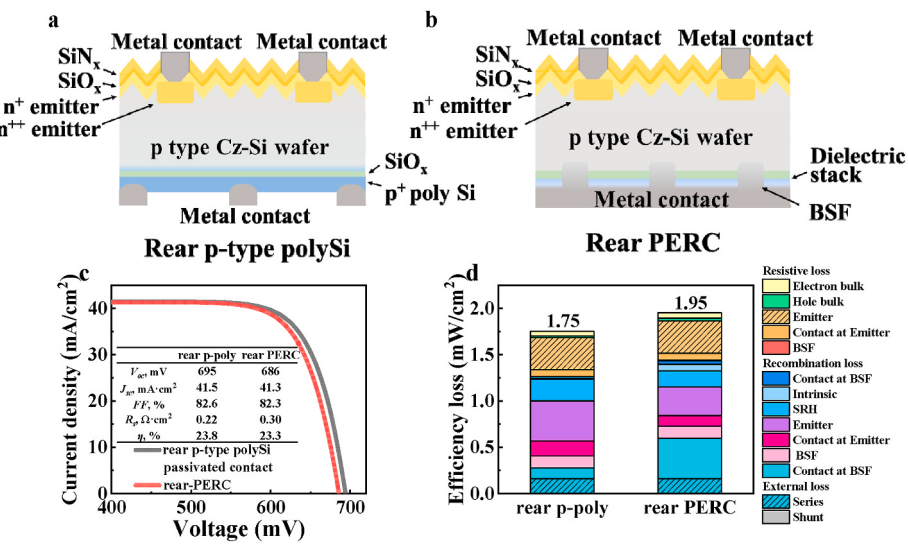


Fig. 6. Sketches of Ga-doped CZ Si solar cells for simulation with (a) p-type polysilicon passivating contact and (b) PERC rear contact. (c) The simulated light I-V curves and (d) the free energy loss analysis (FELA) of the two simulated devices.

Declaration of competing interest

The authors declare that they have no known competing financial interests or personal relationships that could have appeared to influence the work reported in this paper.

Acknowledgements

This work was supported by National Key R&D Program of China (Grant No. 2018YFB1500403), National Natural Science Foundation of China (61974178, 61874177), Ningbo “Innovation 2025” Major Project (2020Z098), Key Research and Development Program of Zhejiang Province (2021C01006), Zhejiang Energy Group (Project No. znkj-2018-118), Youth Innovation Promotion Association (2018333), Zhejiang Provincial Natural Science Foundation (LY19F040002).

References

- [1] A. Herguth, Simulation study on the concept of lifetime-equivalent defect density in the context of light-induced degradation (LID) experiments, in: 2019 IEEE 46th Photovoltaic Specialists Conference (PVSC), IEEE, Chicago, IL, USA, 2019, pp. 54–60, <https://doi.org/10.1109/PVSC40753.2019.8981263>.
- [2] J. Lindroos, H. Savin, Review of light-induced degradation in crystalline silicon solar cells, Sol. Energy Mater. Sol. Cell. 147 (2016) 115–126, <https://doi.org/10.1016/j.solmat.2015.11.047>.
- [3] T. Nieuwelt, J. Schon, W. Warta, S.W. Glunz, M.C. Schubert, Degradation of crystalline silicon due to boron-oxygen defects, IEEE J. Photovolt. 7 (2017) 383–398, <https://doi.org/10.1103/PhysRevLett.93.055504>.
- [4] F. Fertig, R. Lantsch, F. Fröhlauf, F. Kersten, M. Schütze, C. Taubitz, J. Lindroos, J. W. Müller, Excessive light-induced degradation in boron-doped Cz silicon PERC triggered by dark annealing, Sol. Energy Mater. Sol. Cell. 200 (2019) 109968, <https://doi.org/10.1016/j.solmat.2019.109968>.
- [5] S.W. Glunz, S. Rein, J. Knobloch, W. Wetting, T. Abe, Comparison of boron- and gallium-doped p-type Czochralski silicon for photovoltaic application, Prog. Photovoltaics Res. Appl. 7 (1999) 463–469, [https://doi.org/10.1002/\(SICI\)1099-159X](https://doi.org/10.1002/(SICI)1099-159X).
- [6] V. Meemongkolkiat, K. Nakayashiki, A. Rohatgi, G. Crabtree, J. Nickerson, T. L. Jester, Resistivity and lifetime variation along commercially grown Ga- and B-Doped Czochralski Si ingots and its effect on light-induced degradation and performance of solar cells, Prog. Photovoltaics Res. Appl. 14 (2006) 125–134, <https://doi.org/10.1002/pip.659>.
- [7] X. Zhang, W. Liu, Y. Chen, S. Chen, G. Xu, Y. Hu, Y. Yang, D. Chen, Y. Chen, P. P. Altermatt, P.J. Verlinden, Z. Feng, A roadmap towards 24%-efficiency PERC cells based on screen printing for mass production, in: 37th European Photovoltaic Solar Energy Conference and Exhibition, 2019, pp. 233–237, <https://doi.org/10.4229/EUPVSEC20202020-2CO.13.1>.
- [8] F. Feldmann, M.B.C. Reichel, M. Hermle, S.W. Glunz, A passivated rear contact for high-efficiency n-type silicon solar cells enabling high V_{oc} s and FF>82%, in: 28th European Photovoltaic Solar Energy Conference and Exhibition (PVSE) Paris, France, 2013, pp. 988–992, <https://doi.org/10.4229/28thEUPVSEC2013-2CO.4.4>.
- [9] T.G. Allen, J. Bullock, X. Yang, A. Javey, S. De Wolf, Passivating contacts for crystalline silicon solar cells, Nat. Energy. 4 (2019) 914–928, <https://doi.org/10.1038/s41560-019-0463-6>.
- [10] A. Moldovan, F. Feldmann, M. Zimmer, J. Rentsch, J. Benick, M. Hermle, Tunnel oxide passivated carrier-selective contacts based on ultra-thin SiO₂ layers, Sol. Energy Mater. Sol. Cell. 142 (2015) 123–127, <https://doi.org/10.1016/j.solmat.2015.06.048i>.
- [11] F. Haase, F. Kiefer, S. Schäfer, C. Kruse, J. Krügener, R. Brendel, R. Peibst, Interdigitated back contact solar cells with polycrystalline silicon on oxide passivating contacts for both polarities, Jpn. J. Appl. Phys. 56 (2017), 08MB15, <https://doi.org/10.7567/JJAP.56.08MB15>.
- [12] C. Chen, L. Ma, C. Huang, X. Zhang, Z. Wang, C. Chen, S. Zhan, R. Liu, Z. Qiao, Z. Du, Z. Liu, J. Chen, Towards 24% efficiency for industrial n-type bifacial passivating-contact solar cells with homogeneous emitter, in: 37th European Photovoltaic Solar Energy Conference and Exhibition, 2020, pp. 160–163, <https://doi.org/10.4229/EUPVSEC20202020-2AO.6.1>.
- [13] D. Chen, Y. Chen, Z. Wang, J. Gong, C. Liu, Y. Zou, Y. He, Y. Wang, L. Yuan, W. Lin, R. Xia, L. Yin, X. Zhang, G. Xu, Y. Yang, H. Shen, Z. Feng, P.P. Altermatt, P. J. Verlinden, 24.58% total area efficiency of screen-printed, large area industrial silicon solar cells with the tunnel oxide passivated contacts (i-TOPCon) design, Sol. Energy Mater. Sol. Cell. 206 (2020) 110258, <https://doi.org/10.1016/j.solmat.2019.110258>.
- [14] F. Feldmann, M. Simon, M. Bivour, C. Reichel, M. Hermle, S.W. Glunz, Carrier-selective contacts for Si solar cells, Appl. Phys. Lett. 104 (2014) 181105, <https://doi.org/10.1063/1.4875904>.
- [15] S. Mack, J. Schube, T. Fellmeth, F. Feldmann, M. Lenes, J.M. Luchies, Metallisation of boron-doped polysilicon layers by screen printed silver pastes, Phys. Status Solidi RRL. 11 (2017) 1700334, <https://doi.org/10.1002/psrr.201700334>.
- [16] D.L. Young, B.G. Lee, D. Fogel, W. Nemeth, V. LaSalvia, S. Theingi, M. Page, M. Young, C. Perkins, P. Stradins, Gallium-doped poly-Si:Ga/SiO₂ passivated emitters to n-cz wafers with $iV_{oc} > 730$ mV, IEEE J. Photovolt. 7 (2017) 1640–1645, <https://doi.org/10.1109/JPHOTOV.2017.2748422>.
- [17] M.K. Stodolny, J. Anker, C.J.J. Tool, M. Koppes, A.A. Mewe, P. Manshanden, M. Lenes, I.G. Romijn, Novel schemes of p^+ polySi hydrogenation implemented in industrial 6" bifacial front-and-rear passivating contacts solar cells, in: 35th European Photovoltaic Solar Energy Conference and Exhibition, 2018, pp. 414–417, <https://doi.org/10.4229/35thEUPVSEC20182018-2CO.10.3>.
- [18] D. Yan, A. Cuevas, S.P. Phang, Y. Wan, D. Macdonald, 23% efficient p-type crystalline silicon solar cells with hole-selective passivating contacts based on physical vapor deposition of doped silicon films, Appl. Phys. Lett. 113 (2018), 061603, <https://doi.org/10.1063/1.5037610>.
- [19] A. Ingenito, G. Nogay, Q. Jeangros, E. Rucavado, C. Allebé, S. Eswara, N. Valle, T. Wirtz, J. Horzel, T. Koida, M. Morales-Maisi, M. Despeisses, F.J. Haug, P. Löper, C. Ballif, A passivating contact for silicon solar cells formed during a single firing thermal annealing, Nat. Energy. 3 (2018) 800–808, <https://doi.org/10.1038/s41560-018-0239-4>.
- [20] X. Guo, M. Liao, Z. Rui, Q. Yang, Z. Wang, C. Shou, W. Ding, X. Luo, Y. Cao, J. Xu, L. Fu, Y. Zeng, B. Yan, J. Ye, Comparison of different types of interfacial oxides on hole-selective p+-poly-Si passivated contacts for high-efficiency c-Si solar cells, Sol. Energy Mater. Sol. Cell. 210 (2020) 110487, <https://doi.org/10.1016/j.solmat.2020.110487>.
- [21] A. Fell, A free and fast three-dimensional/two-dimensional solar cell simulator featuring conductive boundary and quasi-neutrality approximations, IEEE Trans. Electron. Dev. 60 (2013) 733–738, <https://doi.org/10.1109/TED.2012.2231415>.
- [22] A. Fell, J. Schön, M.C. Schubert, S.W. Glunz, The concept of skins for silicon solar cell modeling, Sol. Energy Mater. Sol. Cell. 173 (2017) 128–133, <https://doi.org/10.1016/j.solmat.2017.05.012>.
- [23] M. Winter, D. Walter, D. Bredemeier, J. Schmidt, Light-induced lifetime degradation effects at elevated temperature in Czochralski-grown silicon beyond boron-oxygen-related degradation Czochralski-grown silicon beyond boron-oxygen-related degradation, Sol. Energy Mater. Sol. Cell. 201 (2019) 110060, <https://doi.org/10.1016/j.solmat.2019.110060>.
- [24] D.C. Walter, B. Lim, J. Schmidt, Realistic efficiency potential of next-generation industrial Czochralski-grown silicon solar cells after deactivation of the boron–oxygen-related defect center, Prog. Photovoltaics Res. Appl. 24 (2016) 920–928, <https://doi.org/10.1002/pip.2731>.
- [25] J. Adey, R. Jones, D.W. Palmer, P.R. Briddon, S. Öberg, Degradation of boron-doped czochralski-grown silicon solar cells, Phys. Rev. Lett. 93 (2004), 055504, <https://doi.org/10.1103/PhysRevLett.93.055504>.
- [26] L. Shao, J. Liu, Q.Y. Chen, W.K. Chu, Boron diffusion in silicon the anomalies and control by point defect engineering, Math. Sci. Eng. R. 42 (2003) 65–114. <https://doi.org/10.1016/j.mser.2003.08.002>.
- [27] S. Choi, J. Baek, T. Kim, K.H. Min, M.S. Jeong, H. Song, M.G. Kang, D. Kim, Y. Kang, H. Lee, J. Myoung, S. Park, Interface analysis of ultrathin SiO₂ layers between c-Si substrates and phosphorus-doped poly-Si by theoretical surface potential analysis using the injection-dependent lifetime, Prog. Photovoltaics Res. Appl. (2020) 3338, <https://doi.org/10.1002/pip.3338>.
- [28] M. Müller, Reporting effective lifetimes at solar cell relevant injection densities, Energy Procedia 92 (2016) 138–144, <https://doi.org/10.1016/j.egypro.2016.07.012>.
- [29] L. Lu, Y. Zeng, M. Liao, J. Zheng, Y. Lin, M. Feng, Y. Zhi, H. He, W. Ding, C. Shou, G. Qin, Baoji Yan, J. Ye, Dopant diffusion through ultrathin AlO_x and AlO_x/SiO_x tunnel layer in TOPCon structure and its impact on the passivation quality on c-Si solar cells, Sol. Energy Mater. Sol. Cell. 223 (2021) 110970, <https://doi.org/10.1016/j.solmat.2021.110970>.
- [30] A.F.W. Willoughby, A.G.R. Evans, P. Champ, K.J. Yallup, D.J. Godfrey, M. G. Dowsett, Diffusion of boron in heavily doped n- and p-type silicon, J. Appl. Phys. 59 (1986) 2392–2397, <https://doi.org/10.1063/1.336340>.
- [31] H. Kodera, Diffusion coefficients of impurities in silicon melt, Jpn. J. Appl. Phys. 2 (1963) 212–219, <http://iopscience.iop.org/1347-4065/2/4/212>.
- [32] R.B. Fair, On the role of self-interstitials in impurity diffusion in silicon, J. Appl. Phys. 51 (1980) 5828, <https://doi.org/10.1063/1.327540>.
- [33] A. Richter, J. Benick, R. Müller, F. Feldmann, C. Reichel, M. Hermle, S.W. Glunz, Tunnel oxide passivating electron contacts as full-area rear emitter of high-efficiency p-type silicon solar cells, Prog. Photovoltaics Res. Appl. 26 (2018) 579–586, <https://doi.org/10.1002/pip.2960>.
- [34] C. Hollemann, F. Haase, S. Schäfer, J. Krügener, R. Brendel, R. Peibst, 26.1%-efficient POLO-IBC cells: quantification of electrical and optical loss mechanisms, Prog. Photovoltaics Res. Appl. 27 (2019) 950–958, <https://doi.org/10.1002/pip.3098>.